

## Controlling the Crystal Growth of Dodecasil 3C by Buffering with DL-Histidine

José J. Seral,<sup>[a]</sup> Santiago Uriel,<sup>[b]</sup> and Joaquín Coronas<sup>\*[a]</sup>

**Keywords:** Crystal growth / Zeolites / Sol–gel / Amino acids

Dodecasil 3C, a pure silica zeolite with an MTN-type structure, was prepared by liquid-phase hydrothermal synthesis in the presence of the amino acid DL-histidine. This compound acts as a buffer and affects the growth of zeolite, in particular its aggregation behaviour and particle size. As a result of the alteration the amino acid exerts on the silica

chemistry in aqueous solution, nucleation was lowered and dodecasil 3C was formed as large, single crystals with sizes up to 140  $\mu\text{m}$ .

(© Wiley-VCH Verlag GmbH & Co. KGaA, 69451 Weinheim, Germany, 2008)

### Introduction

Control of the crystal size and morphology when synthesizing a zeolite is of paramount interest for the purposes of either catalysis<sup>[1,2]</sup> or adsorption,<sup>[3,4]</sup> and also when the objective is obtaining zeolites as fillers for mixed-matrix membranes<sup>[5]</sup> or when preparing<sup>[6]</sup> or crystallizing<sup>[7,8]</sup> a continuous layer of zeolite. Colloidal zeolites<sup>[9,10]</sup> can be used as seeds for growing larger crystals or membranes, and they also have reduced diffusion path lengths. However, they may have inherent problems of pressure drop and safe management due to the possibility of forming respirable aerosols, and their separation from a liquid phase may be complicated. Many of these difficulties have been overcome through the formation of hierarchical pore system materials.<sup>[11–13]</sup> Moreover, large zeolitic crystals can be of interest for structure refining,<sup>[14]</sup> characterization,<sup>[15]</sup> catalytic<sup>[16]</sup> and electronic applications,<sup>[17]</sup> etc.

In the present work, the zeolitic material dodecasil 3C was prepared by liquid-phase hydrothermal synthesis in the presence of the amino acid DL-histidine. This compound, which makes no specific contribution to the growth of the zeolite (in terms of structuring power), acts as a buffer and directly affects the particle size of dodecasil 3C. The advantage of using DL-histidine as a buffer is related to the fact that no additional (to the required tetramethylammonium cation) structuring cations are introduced into the synthesis solution to control the pH during the hydrothermal synthe-

sis. It is well known that alkaline cations may lead at high pH to the formation of hydrated silicates such as kenyaite,<sup>[18]</sup> kanemite<sup>[19]</sup> and magadiite,<sup>[20]</sup> among others.

Zeolites (in a wider sense, nanoporous materials) have always had a fruitful relationship with amino acids. Zeolite beta,<sup>[21,22]</sup> ZSM-5<sup>[21,23]</sup> and zeolite Y<sup>[24]</sup> have been used to adsorb various amino acids from water solutions, founding the fact that amino acids of different polarity can be separated by adjusting the pH of the solution appropriately.<sup>[21]</sup> The adsorption of amino acids onto zeolites is in general dominated by electrostatic interactions,<sup>[24]</sup> although hydrophobic interactions involving nonpolar side groups<sup>[21,23]</sup> and steric<sup>[22]</sup> interactions complete the overall molecule–adsorbent picture.

Concerning the synthesis of nanoporous materials, ordered silica structures have been obtained by the self-assembling of synthetic cysteine–lysine block copolypeptides that mimic the properties of silicatein producing the hydrolysis and aggregation of tetraethoxysilane,<sup>[25]</sup> whereas an anionic surfactant based on the amino acid alanine (*N*-myristoyl-L-alanine sodium salt) has templated the synthesis of chiral mesoporous silica.<sup>[26–28]</sup> In an attempt to approach biomimetic silicification, homopeptides [poly(lysine) and poly(arginine)] have been shown to induce the formation of mesoporous silica.<sup>[29]</sup> To understand the contribution of complex components (proteins) in biosilicification, a number of amino acids have been directly studied in their role as silica polymerizing agents at pH 7.<sup>[30,31]</sup> Also, nanoparticles have been found in unbuffered lysine–silica sols,<sup>[32]</sup> that is, under conditions of high pH common to those employed for templating mesoporous silica.

From a different angle, zeolites catalyze the transformation of amino acids, for example, Ersorb-4 (a clinoptilolite-type zeolite material with a Si/Al ratio of 5), into the appropriate *N*-acyl derivative.<sup>[33]</sup> Zeolite-encapsulated copper(II) amino acid complexes have been prepared for which, upon

[a] Department of Chemical and Environmental Engineering and Nanoscience Institute of Aragon, University of Zaragoza, María de Luna, 3. 50018 Zaragoza, Spain  
Fax: +34-976-761879  
E-mail: coronas@unizar.es

[b] Department of Organic Chemistry, University of Zaragoza, María de Luna, 3. 50018 Zaragoza, Spain

Supporting information for this article is available on the WWW under <http://www.eurjic.org> or from the author.

immobilization, the coordination chemistry is almost identical to that in solution.<sup>[34]</sup> Moreover, DL-histidine has exhibited a key role in the swelling of the porous layered silicate AMH-3.<sup>[35]</sup> Finally, it has been suggested that relatively high silica zeolites (such as mutinaite<sup>[36]</sup> and tschernichite,<sup>[37]</sup> natural analogues of ZMS-5 and zeolite Beta, respectively) played a role in the biochemical evolution that occurred in the early history of the Earth with the incorporation of amino acids into the first primitive proteins.<sup>[38,39]</sup> Zeolites would have been present on Earth in the Archaean aeon, or at the time of early life forms.<sup>[40]</sup>

## Results and Discussion

Table 1 shows some experiments in which dodecasil 3C was prepared under various synthesis conditions, some of them involving the amino acid DL-histidine. Clathrasil dodecasil 3C (the completely siliceous form) and zeolite ZSM-39 are isomorphes sharing an MTN-type structure.<sup>[41]</sup> This crystal structure was proposed by Schelenker et al.<sup>[42]</sup> and refined in detail by Gies.<sup>[43]</sup> The interest in this material has been recently highlighted by its potential optical applications<sup>[44]</sup> and its use as a hydrogen storage medium.<sup>[45]</sup> Also, a metal–organic framework with MTN-type zeolite topology was found in 2005.<sup>[46]</sup> In any event, in this work dodecasil 3C was prepared in the absence of chloride or fluoride species (Table 1), which have been widely used in the synthesis of zeolites, and for this material in particular.<sup>[47–50]</sup> Run 1 in Table 1 corresponds to the preparation of dodecasil 3C under synthesis conditions that could be considered as a blank experiment, without the use of an amino acid. As depicted in Figure 1, and by comparison with the simulated X-ray diffraction pattern,<sup>[41]</sup> this run yields the pure MTN-type zeolitic phase. SEM images a and b in Figure 2, obtained from run 1, show a crystalline material with a tremendous trend to aggregate through intergrowth, so that the crystals in Figure 2b are approximately 20–30  $\mu\text{m}$  in size.

Table 1. Synthesis of dodecasil 3C at 180 °C by using the following molar composition: 3SiO<sub>2</sub>/2TMAOH/xDL-histidine/500H<sub>2</sub>O.

Run	x	Synthesis Time [d]	pH		Product [mg]	
			Before	After	Amorphous	Crystals
1	0	10	11.9	11.6	0	337
2	1	10	11.1	9.8	149	126
3	1	30	11.1	9.9	87	239

Run 2 in Table 1 was performed under the same conditions corresponding to run 1 but by adding to the synthesis solution 1 mol of DL-histidine for each 2 mol of TMAOH. The first effect of the incorporation of the amino acid to the solution is that the pH before the synthesis (measured after 5 h of solution aging upon the complete mixture of all the reactants) was 0.8 pH units below the corresponding value reached without its use. The buffer characteristic of many amino acids is well known. Scheme 1 shows the aqueous dissociation equilibria related to DL-histidine. The

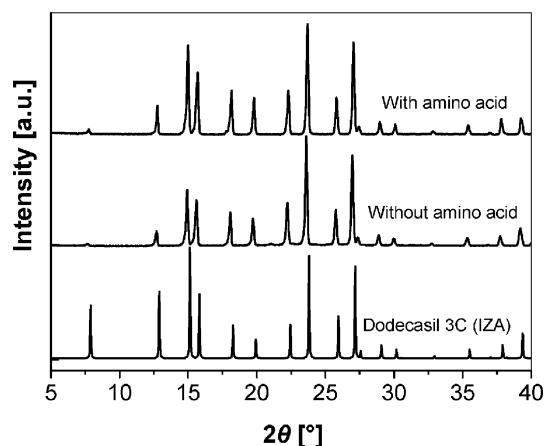


Figure 1. XRD patterns, from bottom to top, of simulated dodecasil 3C<sup>[41]</sup> and crystals obtained at 180 °C, 10 d without and with an amino acid.

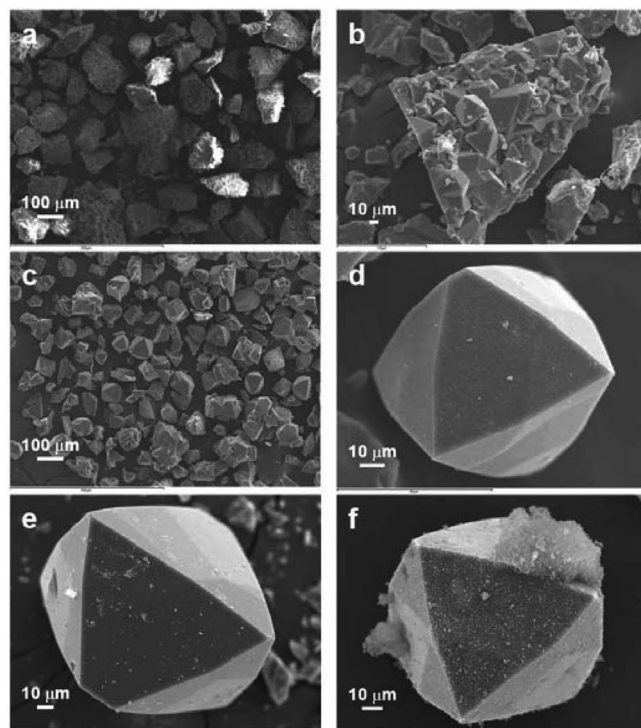
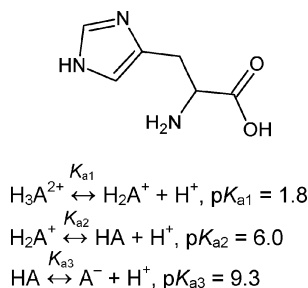


Figure 2. SEM images of dodecasil 3C prepared: (a,b) in the absence of amino acid at 180 °C for 10 d; (c,d) in the presence of amino acid at 180 °C for 10 d (e) and for 30 d. (f) A dodecasil 3C crystal found in the amorphous portion obtained at 180 °C after 10 d.

$pK_a$  values for DL-histidine are 1.8 (for the equilibrium between  $H_3A^{2+}$  and  $H_2A^+$  forms), 6.0 (for the equilibrium between  $H_2A^+$  and HA forms) and 9.3 (for the equilibrium between HA and  $A^-$  forms). Figure S1 (Supporting Information) presents the dissociation degree for DL-histidine as a function of pH. In the range of pH around  $pK_{a3}$  (9.3), the relationship between pH and [HA] and [ $A^-$ ] can be described by the Henderson–Hasselbalch equation  $\{pH = 9.3 + \log([A^-]/[HA])\}$ ,<sup>[51]</sup> which is widely used for estimating the pH of a buffer solution. As the pH values in Table 1 for

the experiments in the presence of DL-histidine are above  $pK_{a3}$ , this means that  $[A^-]$  was higher than  $[HA]$  before and after the synthesis, and this is due to the reaction between HA and the hydroxy groups, as suggested by reaction (a) in Scheme 2. Before continuing with the effect of the amino acid, we must consider reaction (b), the hydrolysis of TEOS, and reaction (c), the dissolution, or properly speaking the deprotonation, of the silica catalyzed by the presence of a strong base, so that when the pH value exceeds about 10.5–11, silica dissolves extensively.<sup>[52]</sup> Now, it can be said that reaction (a) competes for the hydroxy groups with reactions (b) and (c) (all in Scheme 2) with two effects: (i) reducing the pH of the synthesis solution (as discussed), and consequently, (ii) controlling the silica dissolution.



Scheme 1. DL-histidine formula and its dissociation equilibria.

- (a)  $HA + OH^- \rightarrow A^- + H_2O$   
 (b)  $Si(OEt)_4 + 4OH^- \rightarrow Si(OH)_4 + 4EtO^-$   
 (c)  $Si(OH)_4 + OH^- \rightarrow Si(OH)_3O^- + H_2O$   
 (d)  $Si(OH)_4 + A^- \rightarrow Si(OH)_3O^- + HA$   
 (e)  $Si(OH)_3O^- + Si(OH)_4 \rightarrow Si(OH)_3-O-Si(OH)_3 + OH^-$

Scheme 2. (a) Equilibrium between HA and  $A^-$  forms; (b) hydrolysis of TEOS; (c) dissolution of silica in alkaline medium; (d) “dissolution” of silica by the amino acid (regeneration of the zwitterion); (e) condensation reaction.

It seems evident that the reduction of the pH of the solution followed by a diminution of the rate of silica dissolution must exert an important effect on the nucleation process of dodecasil 3C, so that a lower nucleation rate may be expected. Figure 2c when compared to 2a shows the effect of lowering the nucleation rate through the addition of the amino acid, producing scarcely agglomerated, large dodecasil 3C crystals: there was a smaller amount of nuclei to consume the same nutrients. Many of the particles in Figure 2c are single crystals of dodecasil 3C of about 60–70  $\mu m$  in size (see Figure 2d). Figure 2e demonstrates how dodecasil 3C crystals can be even larger (about 130–140  $\mu m$  in size) after 30 d of hydrothermal synthesis (Table 1, run 3), when compared to those obtained after 10 d. Similarly to the zeolite crystal growth established here, Vergilov and Valtchev observed that, in the case of ZSM-39, by using  $TMA^+$  only, complex crystal twins were formed, whereas the addition of  $TrMA^+$  (trimethylammonium) led to the synthesis of large octahedral monocrystals.<sup>[47]</sup> The larger size of the crystals prepared with amino acid translates into a more difficult

removal of the template because of mass and heat transport limitations (see Figure S2, Supporting Information). As a collateral effect, some amorphous (see Table 1) is produced in the crystallization experiments in the presence of amino acid, although the amorphous material decreased from 149 to 87 mg as the synthesis time augmented from 10 to 30 d. Figure 2f corresponds to a dodecasil 3C crystal found in the amorphous portion collected from run 2 (see Table 1).

Returning to Scheme 2, reaction (d), in which anionic DL-histidine ( $A^-$ ) reacts with silica to form the zwitterionic species (HA), would contribute to keep the buffering character of the crystallization medium, and hence, the pH close to the value of  $pK_{a3}$ . Note that reactions (c) and (d) have the same effect in terms of silica dissolution or mineralization, giving rise to one  $Si(OH)_3O^-$  species for each of either  $A^-$  or  $OH^-$ , respectively. However, reaction (d) is produced to a lesser extent than reaction (b), and does not compensate for the loss of the hydroxy groups by the reaction with the amino acid. The effect of the amino acid on the silica mineralization would otherwise not be appreciable, as the sum of reactions (a) and (d) would be equal to reaction (c) if both reactions occurred to the same degree.

To gain insight into the effect of the amino acid on the synthesis solution before being autoclaved, the ion conductivities of two solutions, with and without amino acid, were monitored as a function of time, as shown in Figure 3. When after 300 s TMAOH was added to the DL-histidine solution (A), the conductivity reached a constant value of about 26.4  $mS\,cm^{-1}$ . The corresponding value measured for the solution without amino acid (B) was 43.4  $mS\,cm^{-1}$ . These values indicate the consumption of  $OH^-$  groups by the amino acid, as the conductivity of the hydroxy group must be higher than that of the anionic amino acid (e.g.,  $OH^-$  conductivity is about six times higher than that of  $C_6H_5COO^-$ ) and perhaps the formation of a  $TMA^+A^-$  ion pair. Upon the addition of TEOS, hydrolysis and dissolution reactions catalyzed by  $OH^-$  groups dramatically decreased the conductivity. This decrease is considerably slower in the presence of the amino acid. Note that after 2100 s there was for solution A an appreciable additional diminution in the conductivity, probably due to desorption

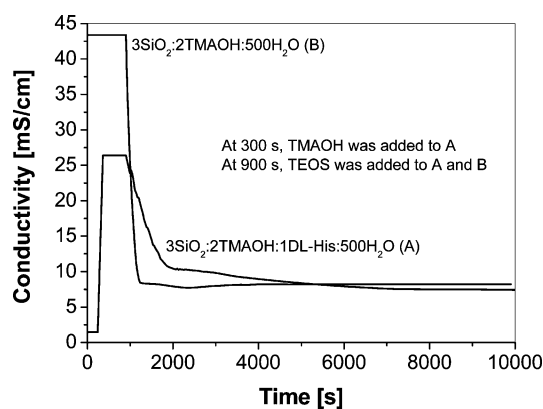


Figure 3. Ion conductivity as a function of time obtained at 20 °C for solutions A (with amino acid) and B (without amino acid).



from the liquid of ethanol byproduct. For solution B, after the sharp initial decrease ending at 1260 s, a weak minimum appeared, indicating some extent of the condensation process (Scheme 2, reaction e),<sup>[53]</sup> which would in part compensate for the expected decrease in the conductivity by releasing hydroxy ions.<sup>[54]</sup> The presence of the amino acid in solution A would hinder the start of the condensation process, and this would determine the zeolite growth, even though the stability of the amino acid was affected by the hydrothermal conditions, as is mentioned in the Experimental Section.

## Conclusions

The addition of the amino acid DL-histidine to the parent gel used for synthesizing dodecasil 3C alters the silica chemistry in aqueous solution, which promotes crystal growth over nucleation. The control over the global crystallization process achieved under these conditions allows us to obtain large, single crystals of dodecasil 3C up to 140  $\mu\text{m}$  in size. We believe that this growing strategy could be applied to other zeolites, perhaps by using the less expensive L-amino acid form.

## Experimental Section

Dodecasil 3C was obtained by using the following general molar composition:  $3 \text{ SiO}_2/2 \text{ TMAOH}/x \text{ DL-histidine}/500 \text{ H}_2\text{O}$ , where  $x = 1$  or 0 (blank experiment). Tetraethylorthosilicate (TEOS), +98 wt.-%, and tetramethylammonium hydroxide (TMAOH), 25 wt.-% (in water), both supplied by Fluka, were chosen as the silica precursor and the structure-directing agents, respectively. DL-histidine, 99+ wt.-%, was also purchased from Fluka. In a typical synthesis, to prepare approximately 30 mL of reaction gel, DL-histidine (0.477 g) was dissolved in deionized water (25.741 g) by heating whilst stirring up to 75 °C. Afterwards, the resulting solution was cooled and maintained at room temperature. Next, TMAOH commercial solution (2.221 g) was mixed with the amino acid solution with continuous stirring. Finally, TEOS (1.942 g) was added to the above mixture, which was then vigorously stirred for 5 h to give rise to a one-phase, clear and colourless solution. The solution was poured into a Teflon-lined autoclave, where the hydrothermal synthesis was carried out at 180 °C for 10 or 30 d. The synthesis was terminated by cooling the autoclave to room temperature in still air. When amino acid is present in the formulated synthesis solution, the transparent liquid collected when opening the autoclave is brownish (colourless without amino acid) and displays some suspended amorphous material, and crystals remain weakly stuck to the Teflon-lining. This circumstance allows easy and clean separation of the crystals, which were washed with deionized water (200 mL). The powders obtained were dried at 100 °C for 2 d.

The materials were characterized by scanning electron microscopy (SEM, JEOL JSM-6400) and X-ray diffraction (Rigaku/Max System diffractometer,  $\text{Cu-K}\alpha$  radiation,  $\lambda = 1.5418 \text{ \AA}$ , and graphite monochromator). Thermogravimetric analyses were carried out in air atmosphere up to 1000 °C with a heating rate of  $10 \text{ }^\circ\text{C min}^{-1}$  by using Mettler-Toledo equipment (TGA/SDTA851<sup>e</sup>). Also, it was confirmed (not shown) by  $^1\text{H}$  NMR (Bruker Avance 400 spectrometer at 9.4 T and 400.13 MHz) that the amino acid decomposed

during the hydrothermal synthesis, even though it carried out its role as a buffer.

**Supporting Information** (see footnote on the first page of this article): The dissociation degree for DL-histidine as a function of pH; the TGA weight losses for dodecasil 3C crystals synthesized at 180 °C and for 10 d without and with amino acid.

## Acknowledgments

Financing from the Spanish Ministry of Science and Innovation (MAT2007-61028) is gratefully acknowledged.

- [1] U. Wilkenhoner, G. Langhendries, F. van Laar, G. V. Baron, D. W. Gammon, P. A. Jacobs, E. van Steen, *J. Catal.* **2001**, *203*, 201–212.
- [2] G. Li, S. C. Larsen, V. H. Grassian, *Catal. Lett.* **2005**, *103*, 23–32.
- [3] D. M. Ruthven, B. K. Kaul, *Ind. Eng. Chem. Res.* **1993**, *32*, 2053–2057.
- [4] J. H. Kim, T. Kunieda, M. Niwa, *J. Catal.* **1998**, *173*, 433–439.
- [5] S. C. Byun, Y. J. Jeong, J. W. Park, S. W. Kim, H. Y. Ha, W. J. Kim, *Solid State Ion.* **2006**, *177*, 3233–3243.
- [6] L. Tosheva, V. P. Valtchev, B. Mihailova, A. M. Doyle, *J. Phys. Chem. C* **2007**, *111*, 12052–12057.
- [7] W. C. Wong, L. T. Y. Au, P. P. S. Lau, C. T. Ariso, K. L. Yeung, *J. Membr. Sci.* **2001**, *193*, 141–161.
- [8] Z. P. Lai, M. Tsapatsis, J. R. Nicolich, *Adv. Funct. Mater.* **2004**, *14*, 716–729.
- [9] A. E. Persson, B. J. Schoeman, J. Sterte, J.-E. Otterstedt, *Zeolites* **1994**, *14*, 557–567.
- [10] S. Mintova, N. H. Olson, V. Valtchev, T. Bein, *Science* **1999**, *283*, 958–960.
- [11] C. C. Pavel, W. Schmidt, *Chem. Commun.* **2006**, 882–884.
- [12] M. Hartmann, *Angew. Chem. Int. Ed.* **2004**, *43*, 5880–5882.
- [13] V. Sebastian, I. Diaz, C. Tellez, J. Coronas, J. Santamaria, *Adv. Funct. Mater.* **2008**, *18*, 1314–1320.
- [14] X. Q. Wang, A. J. Jacobson, *Chem. Commun.* **1999**, 973–974.
- [15] M. Vilaseca, E. Mateo, L. Palacio, P. Pradanos, A. Hernandez, A. Paniagua, J. Coronas, J. Santamaria, *Microporous Mesoporous Mater.* **2004**, *71*, 33–37.
- [16] Z. A. D. Lethbridge, J. J. Williams, R. I. Walton, K. E. Evans, C. W. Smith, *Microporous Mesoporous Mater.* **2005**, *79*, 339–352.
- [17] T. Kida, K. Kojima, H. Ohnishi, G. Guan, A. Yoshida, *Ceram. Int.* **2004**, *30*, 727–732.
- [18] F. X. Feng, K. J. Balkus, *Microporous Mesoporous Mater.* **2004**, *69*, 85–96.
- [19] D. C. Apperley, M. J. Hudson, M. T. J. Keene, J. A. Knowles, *J. Mater. Chem.* **1995**, *5*, 577–582.
- [20] U. Brenn, W. Schwieger, K. Wutlig, *Colloid Polym. Sci.* **1999**, *277*, 394–399.
- [21] S. Munsch, M. Hartmann, S. Ernst, *Chem. Commun.* **2001**, 1978–1979.
- [22] J. E. Krohn, M. Tsapatsis, *Langmuir* **2005**, *21*, 8743–8750.
- [23] E. Titus, A. K. Kalkar, V. G. Gaikar, *Colloids Surf. A* **2003**, *223*, 55–61.
- [24] R. Wijnje, H. Bosch, A. B. de Haana, P. J. T. Bussmann, *J. Chromatograph. A* **2007**, *1142*, 39–47.
- [25] J. N. Cha, G. D. Stucky, D. E. Morse, T. J. Deming, *Nature* **2000**, *403*, 289–292.
- [26] S. Che, A. E. Garcia-Bennett, T. Yokoi, K. Sakamoto, H. Kunieda, O. Terasaki, T. Tatsumi, *Nat. Mater.* **2003**, *2*, 801–805.
- [27] S. Che, Z. Liu, T. Ohsuna, K. Sakamoto, O. Terasaki, T. Tatsumi, *Nature* **2004**, *429*, 281–284.
- [28] H. Jin, Z. Liu, T. Ohsuna, O. Terasaki, Y. Inoue, K. Sakamoto, T. Nakanishi, K. Ariga, S. Che, *Adv. Mater.* **2006**, *18*, 593–596.
- [29] T. Coradin, O. Durupthy, J. Livage, *Langmuir* **2002**, *18*, 2331–2336.

- [30] T. Coradin, J. Livage, *Colloids Surf. B* **2001**, *21*, 329–336.
- [31] D. Belton, G. Paine, S. V. Patwardhan, C. C. Perry, *J. Mater. Chem.* **2004**, *14*, 2231–2241.
- [32] T. M. Davis, M. A. Snyder, J. E. Krohn, M. Tsapatsis, *Chem. Mater.* **2006**, *18*, 5814–5816.
- [33] Z. Hell, A. Cwik, S. Finta, Z. Horvath, *J. Mol. Catal. A* **2002**, *184*, 191–195.
- [34] B. M. Weckhuysen, A. A. Verberckmoes, L. Fu, R. A. Schoonheydt, *J. Phys. Chem.* **1996**, *100*, 9456–9461.
- [35] S. Choi, J. Coronas, E. Jordan, W. Oh, S. Nair, F. Onorato, D. F. Shantz, M. Tsapatsis, *Angew. Chem. Int. Ed.* **2008**, *47*, 552–555.
- [36] E. Galli, G. Vezzalini, S. Quartieri, A. Alberti, M. Franzini, *Zeolites* **1997**, *19*, 318–322.
- [37] J. V. Smith, J. J. Pluth, R. C. Boggs, D. G. Howard, *J. Chem. Soc., Chem. Commun.* **1991**, 363–364.
- [38] J. V. Smith, *Proc. Natl. Acad. Sci. USA* **1998**, *95*, 3370–3375.
- [39] J. V. Smith, F. P. Arnold, I. Parsons, M. R. Lee, *Proc. Natl. Acad. Sci. USA* **1999**, *96*, 3479–3485.
- [40] E. G. Nisbet, N. H. Sleep, *Nature* **2001**, *409*, 1083–1091.
- [41] Ch. Baerlocher, L. B. McCusker, Database of Zeolite Structures: <http://www.iza-structure.org/databases/>.
- [42] J. L. Schlenker, F. G. Dwyer, E. E. Jenkins, W. J. Rohrbaugh, G. T. Kokotailo, W. M. Meier, *Nature* **1981**, *294*, 340–342.
- [43] H. Gies, *Z. Kristallogr.* **1984**, *167*, 73–82.
- [44] H. K. Chae, W. G. Klemperer, D. A. Payne, C. T. A. Suchicital, D. R. Wake, S. R. Wilson in *Materials for Nonlinear Optics*, ACS Symposium Series No. 455 (Eds: S. R. Marder, J. E. Sohn, G. D. Stucky), American Chemical Society, Washington, DC, **1991**, p. 528.
- [45] A. W. C. van den Berg, E. Flikkema, J. C. Jansen, S. T. Bromley, *J. Chem. Phys.* **2005**, *122*, 204710.
- [46] Q. R. Fang, G. S. Zhu, M. Xue, J. Y. Sun, Y. Wei, S. L. Qiu, R. R. Xu, *Angew. Chem. Int. Ed.* **2005**, *44*, 3845–3848.
- [47] I. Vergilov, V. Valtchev, *Zeolites* **1991**, *11*, 387–390.
- [48] S. J. Weigel, J. C. Gabriel, E. G. Puebla, A. M. Bravo, N. J. Henson, L. M. Bull, A. K. Cheetham, *J. Am. Chem. Soc.* **1996**, *118*, 2427–2435.
- [49] U. Deforth, K. K. Unger, F. Schuth, *Microporous Mater.* **1997**, *9*, 287–290.
- [50] J. Dong, X. Tong, J. Yu, H. Xu, L. Liu, J. Li, *Mater. Lett.* **2008**, *62*, 4–6.
- [51] H. N. Po, N. M. Senozan, *J. Chem. Educ.* **2001**, *78*, 1499–1503.
- [52] D. W. Breck, *Zeolite Molecular Sieves*, Wiley, New York, **1974**, p. 338.
- [53] C. J. Brinker, G. W. Scherer, *Sol-Gel Science: The Physics and Chemistry of Sol-Gel Processing*, Academic Press, San Diego, **1990**, p. 145.
- [54] A. Navrotsky, *Curr. Opin. Colloid Interface Sci.* **2005**, *10*, 195–202.

Received: July 10, 2008

Published Online: September 25, 2008